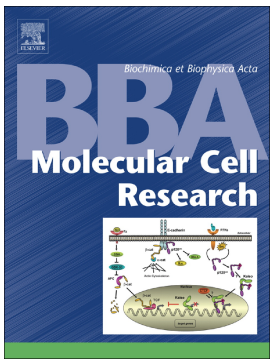

Role of AGAP2 in the profibrogenic effects induced by TGFβ in LX-2 hepatic stellate cells

Amaia Navarro-Corcuera, María J. López-Zabalza, Juan J. Martínez-Irujo, Gloria Álvarez-Sola, Matías A. Ávila, María J. Iraburu, Eduardo Ansorena, Cristina Montiel-Duarte

PII: S0167-4889(18)30410-5
DOI: https://doi.org/10.1016/j.bbamcr.2019.01.008
Reference: BBAMCR 18427

To appear in: *BBA - Molecular Cell Research*

Received date: 1 October 2018
Revised date: 21 December 2018
Accepted date: 14 January 2019

Please cite this article as: Amaia Navarro-Corcuera, María J. López-Zabalza, Juan J. Martínez-Irujo, Gloria Álvarez-Sola, Matías A. Ávila, María J. Iraburu, Eduardo Ansorena, Cristina Montiel-Duarte , Role of AGAP2 in the profibrogenic effects induced by TGFβ in LX-2 hepatic stellate cells. Bbamcr (2019), https://doi.org/10.1016/j.bbamcr.2019.01.008

Title

Role of AGAP2 in the profibrogenic effects induced by TGFβ in LX-2 hepatic stellate cells

Authors

Amaia Navarro-Corcuera[1], María J. López-Zabalza[1], Juan J. Martínez-Irujo[1], Gloria Álvarez-Sola[2,3], Matías A. Ávila[2,3], María J. Iraburu[1], Eduardo Ansorena[#1,3*], Cristina Montiel-Duarte[4 *]

[1] Department of Biochemistry and Genetics, University of Navarra, 31008 Pamplona, Spain

[2] Hepatology Program. CIMA, University of Navarra, Pamplona, Spain.

[3] IdiSNA, Navarra Institute for Health Research, Spain

[4] College of Science and Technology, Nottingham Trent University, Nottingham, UK

[*]Authors contributed equally to the paper

[#]*Corresponding author:* Dr. Eduardo Ansorena, Department of Biochemistry and Genetics, School of Science, University of Navarra, Irunlarrea 1, 31008 Pamplona, Navarra, (Spain). Tel: +34-948-425600 (Ext. 806555). Email: eansorena@unav.es

ORCID ID

Amaia Navarro-Corcuera: 0000-0001-6026-8285; anavarro.1@alumni.unav.es

María J. Iraburu: 0000-0003-3323-7920; miraburu@unav.es

Gloria Álvarez-Sola; **galvarez.1@alumni.unav.es**

Matías A. Ávila; **maavila@unav.es**

María J. López Zabalza: 0000-0002-4778-3319; mjlopez@unav.es

Juan J. Martínez Irujo: 0000-0003-4576-8139; jjmirujo@unav.es

Eduardo Ansorena: 0000-0002-1517-7859; eansorena@unav.es

Cristina Montiel-Duarte: 0000-0002-9144-8809; cristina.montielduarte@ntu.ac.uk

Abstract

Liver damage induces hepatic stellate cells (HSC) activation, characterised by a fibrogenic, proliferative and migratory phenotype. Activated HSC are mainly regulated by transforming growth factor β 1 (TGFβ1), which increases the production of extracellular matrix proteins (*e.g.* collagen-I) promoting the progression of hepatic fibrosis. AGAP2 (ArfGAP with GTPase domain, ankyrin repeat and PH domain 2) is a GTPase/GTP-activating protein involved in the actin remodeling system and receptor recycling. In the present work the role of AGAP2 in human HSC in response to TGFβ1 was investigated. LX-2 HSC were transfected with AGAP2 siRNA and treated with TGFβ1. AGAP2 knockdown prevented to some extent the proliferative and migratory TGFβ1-induced capacities of LX-2 cells. An array focused on human fibrosis revealed that AGAP2 knockdown partially prevented TGFβ1-mediated gene expression of the fibrogenic genes *ACTA2, COL1A2, EDN1, INHBE, LOX, PDGFB, TGFB12*, while favored the expression of *CXCR4, IL1A, MMP1, MMP3 and MMP9 genes.* Furthermore, TGFβ1 induced AGAP2 promoter activation and its protein expression in LX-2. In addition, AGAP2 silencing affected TGFβ1-receptor 2 (TGFR2) trafficking in U2OS cells, blocking its effective recycling to the membrane. AGAP2 silencing in LX-2 cells prevented the TGFβ1-induced increase of collagen-I protein levels, while its over-expression enhanced collagen I protein expression in the presence or absence of the cytokine. AGAP2 overexpression also increased focal adhesion kinase (FAK) phosphorylated levels in LX-2 cells. FAK and MEK1 inhibitors prevented the increase of collagen-I expression caused by TGFβ1 in LX-2 overexpressing AGAP2. In summary, the present work shows for the first time, that AGAP2 is a potential new target involved in TGFβ1 signalling, contributing to the progression of hepatic fibrosis.

Keywords: AGAP2, TGFβ1, hepatic stellate cells, hepatic fibrosis, collagen type I.

Abbreviations:

AGAP2	ArfGAP with GTPase-like domain, ankyrin repeat and PH domain 2
AP-1	Adaptor protein 1
COL-I	Collagen type I
ECM	Extracellular matrix
ERK	Extracellular-signal-regulated kinase
FAK	Focal adhesion kinase
HSC	Hepatic stellate cells
PEI	Polyethylenimine
TGFβ1	Transforming growth factor β1
TGFR2	TGFβ receptor II

1. Introduction

AGAP2 (ArfGAP with GTPase-like domain, ankyrin repeat and PH domain 2) also referred to as PIKE-A (phosphatidylinositol 3-kinase enhancer A), is a member of a family of proteins first described as nuclear GTPases which enhance and maintain protein kinase B (Akt) activity [1-3]. While the initial isoforms characterised are brain specific, AGAP2 seems to be widely expressed in humans and is present in several cellular compartments and in different organs and tissues. AGAP2 does not interact with PI3-kinase. However, when is bound to GTP, is able bind to the active form of Akt, promoting its activity [2]. Together with its role as Akt regulator, in the last years several reports point to AGAP2 as part of the actin remodelling system and being involved in the control of integrin adhesion complexes [3]. AGAP2 has also been linked to internal cell trafficking processes and it was been suggested that could contribute to the trafficking of focal adhesion components to the cell membrane [4]. Some studies have reported that AGAP2 also participates in the very early steps of retrograde sorting between early endosomes and the trans-Golgi network. As such, AGAP2 binds to the clathrin adaptor protein AP-1 promoting the fast recycling of the transferrin receptor [5] and has been shown to regulate the recycling of β2-adrenergic receptors [6].

Interestingly, AGAP2 is overexpressed in several human cancers, including glioblastoma and prostate cancer [9-11]. Moreover, AGAP2 has been described as a proto-oncogene which contributes to tumorigenesis, promoting cell proliferation, migration and invasion [12-14], and could also be involved in tumour growth through the prevention of apoptosis, since its overexpression inhibits apoptosis and its knockdown results in enhanced apoptosis of tumour cell lines [15, 16]. While these data point to an implication of AGAP2 in cancer, its role in other pathophysiological processes has not been fully explored.

Hepatic fibrosis is a determinant condition for the progression to chronic liver disease. About 80% of chronic hepatic fibrosis cases eventually progress to cirrhosis and hepatocellular carcinoma [11]. One of the main cell types responsible for liver fibrosis are activated hepatic stellate cells (HSC), which are liver pericytes that store vitamin A in the normal liver. HSC activation caused by liver injury results in a pro-fibrogenic phenotype characterised by proliferative and migratory properties as well as by a high production of collagen type I, fibronectin and other extracellular matrix (ECM) proteins [18, 19]. Transforming growth factor β (TGFβ) is the main pro-fibrogenic cytokine involved in HSC regulation, promoting their activation and increasing the production and secretion of ECM proteins, and regulating enzymes like metalloproteinases, also key modulators of fibrogenesis [20, 21]. TGFβ exerts its actions through binding to

serine/threonine kinase transmembrane TGFβ receptor I and II (TGFR1 and TGFR2, respectively) which are internalised into the cells via clathrin-coated vesicles. Besides the canonical pathway through Smads, TGFβ also triggers other signalling cascades referred to as “non-canonical pathways”, through mitogen-activated protein kinases (MAPKs), small GTPases or phosphatidylinositol-3-kinase (PI3K)/Akt promoting fibrotic effects [22, 23].

Considering the effects exerted by AGAP2 in other diseases and the molecular and cellular events that characterise the fibrotic process, we sought to understand the relevance and role(s) of AGAP2 in some key mediators of liver fibrogenesis. The aim of the present work was to investigate, for the first time, the potential involvement of AGAP2 in the pro-fibrogenic phenotype of hepatic stellate cells in response to TGFβ.

2. Material and methods

2.1 Cell lines, reagents and antibodies

The LX-2 cell line, an immortalised human hepatic stellate cell line (Merck, Darmstadt, Germany) was cultured in high glucose DMEM supplemented with 2% heat-inactivated fetal bovine serum (FBS) and 1% penicillin/streptomycin (5,000 U/mL) (Lonza, Basel, Switzerland). The human osteosarcoma cell line U2OS cell line (Sigma-Aldrich, St. Louis, MO, USA) was cultured in high glucose DMEM supplemented with 10% heat-inactivated FBS, 2 mM L-glutamine and 1% penicillin/streptomycin (5,000 U/mL) (Lonza, Basel, Switzerland). Cells were cultured in a 5% CO_2 humidified atmosphere at 37°C. The plastic and cell culture reagents were from Sarstedt (Nümbrecht, Germany) and Thermo Fisher Scientific (Waltham, MA, USA).

All general reagents were from Sigma unless otherwise indicated. Recombinant human TGFβ1 was purchased from R&D Systems (Minneapolis, MN, USA), mitomycin A and control siRNA from Santa Cruz Biotechnology (Santa Cruz, CA, USA). AGAP2 siRNA (s42091) was purchased from Ambion (Austin, TX, USA). Focal adhesion kinase (FAK) inhibitor (PF-573228) and polyethylenimine (PEI) from Sigma-Aldrich (St. Louis, MO, USA). The MEK/ERK inhibitor (PD098059) was purchased from Calbiochem (Darmstadt, Germany). jetPRIME transfection reagent was purchased from Polyplus (Illkirch, France), SNAP-cell Oregon Green substrate was obtained from New England Biolabs (Ipswich, MA, USA), and NucBlue Live ReadyProbes Reagent was purchased from Thermo Fisher Scientific (Waltham, MA, USA).

The antibodies used in this study were the following: anti-AGAP2 (anti-PIKE (G-9), sc-166864, anti-MMP-1 (3B6) (sc-21731), anti-MMP-9 (7-11C) (sc-13520), anti-smooth muscle actin (CGA7) (sc-53015) and anti-phospho-FAK (Tyr 397) (sc-11765-R) from Santa Cruz Biotechnology (Santa Cruz, CA, USA); anti-LOX (ab-31238) from Abcam (Cambridge, UK); anti-procollagen I (C2456) and anti-β-actin (A5441) from Sigma-Aldrich (St. Louis, MO, USA); anti-FAK (#3285), anti-mouse IgG (#7076), HRP-linked antibody and anti-rabbit IgG (#7074), HRP-linked antibody from Cell Signalling Technology (Beverly, MA, USA).

2.2 Cellular knock-down

LX-2 cells were transfected with scramble or AGAP2 siRNA. Briefly, cells were seeded with DMEM in plates at the cell density indicated in each case. Non-selective or selective (for AGAP2) knock-down was achieved using 5 nM of scramble or AGAP2 siRNA, respectively, according to the Lipofectamine RNAiMAX Transfection Reagent´s

instructions. The transfection procedure was carried out twice, at the time of seeding and 24 h later.

2.3 Cellular impedance assay

Cell proliferation, morphology change, and attachment quality were monitored with the non-invasive real-time cell analysis (RTCA) iCELLigence instrument (ACEA Biosciences, San Diego, CA, USA). LX-2 cells were seeded at a density of 12.5 x 10^3 cells/well (in 100 μl serum-free DMEM) in an 8-well E-Plate and cellular knock-down using scramble or AGAP2 siRNA was performed. After 43 h, the culture media was replaced with fresh serum-free DMEM. After 6 h of serum starvation, cells were treated with/without 8 ng/ml of TGFβ1. Cell Index (CI) values were measured every hour after cell seeding for a total time of 90 h. For analysis, baseline corrections were carried out subtracting the CI obtained from scramble siRNA-transfected cells. CI values were normalised to the CI at the time immediately prior to TGFβ1 addition for each treatment.

2.4 Cell Proliferation assay

Cell proliferation was studied using the IncuCyte S3 Live-Cell Analysis System from Essen Bioscience (Ann Arbor, MI, USA). After LX-2 cells were transfected with scramble or AGAP2 siRNA as described above, 6 x 10^3 cells/well were seeded in Corning 96-well plate (Sigma-Aldrich, St. Louis, MO, USA), in 100 μl serum-free DMEM. The plate was incubated overnight at 37°C according to manufacturer's instructions. Some wells received 8 ng/ml of TGFβ1 and live cell proliferation was visualised every 4 h for 72 h using a 10x objective. Results are presented as a percentage of confluence using the IncuCyte S3 Live-Cell analysis system software.

2.5 Wound-healing assay

Scratch wound migration assay was performed using IncuCyte S3 Live-Cell Analysis System from Essen Bioscience (Ann Arbor, MI, USA). LX-2 cells were transfected with scramble or AGAP2 siRNA as described above and after 48 h the cells were seeded at 2.5 x 10^4 cells per well in 96-well ImageLock plates (Essen Bioscience, Ann Arbor, MI, USA), in 100 μl serum-free DMEM. Cells were pre-treated with 10 μM mitomycin A for 2 h to inhibit cell proliferation and then uniform cell-free zones were generated employing the WoundMaker 96-pin tool (Essen Bioscience, Ann Arbor, MI, USA). Cells were washed and treated or not with 8 ng/ml TGFβ1. Wound closure images were automatically acquired and registered every 2 h for 48 h. Relative wound density

(expressed as a percentage) and wound width were analysed using the IncuCyte S3 Live-Cell analysis system software.

2.6 Gene expression analysis

LX-2 cells were seeded in a 6-well at a density of 1.5 x 10^5 cells per well in 2 ml DMEM and transfected with scramble or AGAP2 siRNA as described above. After treatment with or without TGFβ1, total RNA was extracted using RNAqueous-Micro Total RNA Isolation Kit (Ambion, Austin, TX, USA) following the manufacturer's instructions. Total RNA was quantified using NanoDrop 8000 spectrophotometer (Thermo Scientific, Waltham, MA, USA). Gene expression changes induced by the selective and non-selective cellular knock-down were analyzed employing 0.8 μg of total RNA using the RT2 First Strand Kit and the human fibrosis RT2 Profiler PCR Array (Qiagen, Hilden, Germany) on the StepOnePlus™ real-time PCR System (Applied Biosystems, Foster City, CA, USA). All data were normalised to an average of three housekeeping genes: β-2 microglobulin (*B2M*), hypoxanthine-guanine phosphoribosyl transferase 1 (*HPRT1*), ribosomal protein, large P0 (*RPLP0*) and glyceraldehyde 3-phosphate dehydrogenase (*GAPDH*). Relative gene expression was obtained using the ΔCt calculation [18].Two PCR arrays per treatment were performed and AGAP2 knock-down was confirmed by Western-blotting.

2.7 Western-blotting

Intracellular proteins were extracted employing radioimmunoprecipitation assay (RIPA) buffer (150 mM sodium chloride, 1.0% Triton x-100, 0.5% sodium deoxycholate, 0.1% sodium dodecyl sulphate (SDS), 50 mM Tris, pH=8.0, supplemented with 1X protease inhibitor cocktail) and protein concentration of the samples was determined by bicinchoninic acid (BCA) assay (Thermo Fisher Scientific, Rockford, IL, USA). Equal amounts of protein (40 μg) were electrophoresed in 8-12% SDS-polyacrylamide gels and transferred onto nitrocellulose membranes (Labtech International LTD, Heathfield, UK). Membranes were incubated with 5% BSA or non-fat dried milk 0.1% Tween20 Tris buffered saline (TBS-T) blocking solution at room temperature for 1 h and then with specific primary antibodies at 4 °C overnight and with a secondary monoclonal anti-mouse IgG or anti-rabbit IgG antibody conjugated to horseradish peroxidase. Immunoreactive protein bands were detected using the Clarity Western ECL Blotting substrate kit (Bio-Rad, Hercules, California, CA, USA) and the intensity of the signal was visualized using FUJIFILM luminescent image analyser LAS-4000. Protein bands were quantified by AIDA analyser v.4.03 software (Tokyo, Japan).

2.8 Plasmids and plasmid construction

pCMV6-Entry mammalian vector with the C-terminal Myc-DDK Tag (4.9 kb) or pCMV6 plasmid containing the AGAP2 (NM_014770) human cDNA ORF Clone (Myc-DDK-tagged) (7.4 kb) were obtained from Origene (Rockville, MD, USA); pGL4.10 was purchased from Promega (Madison, WI, USA). The luciferase-promoterless pGL4.10 vector was purchased from Promega (Madison, WI, USA) and the construction of luciferase-promoterless pGL4.10 vector carrying a ~1000 bp upstream transcription start site (TSS) for AGAP2 referred as *AGAP2*-luc is described elsewhere [19]. The TGFβ-receptor 2 (TGFR2)-SNAP fusion plasmid generated in this study was constructed using pCMV5B-TGFbeta receptor II wt (a gift from Dr. Massague & Jeff Wrana (Addgene plasmid # 11766) [20], and the pSNAPf vector purchased from New England Biolabs (Ipswich, MA, USA).

2.9 Luciferase reporter assay

The possible role of TGFβ1 in the transcriptional rate of AGAP2 promoter in the LX-2 cell line was analysed using the Dual-Light Luciferase & β-Galactosidase System from Applied Biosystems (Foster City, CA, USA). This system is a chemiluminescent reporter gene assay system based on the combined detection of Luciferase and β-Galactosidase. LX-2 cells were seeded at a density of 5 $x10^4$ per well in 24-well plate in 500 μl DMEM. The transfections were performed 24 h later using jetPRIME transfection reagent (Polyplus, Illkirch, France) following the manufacturer's instructions, with 0.5 μg of pGL4.10 (Promega, Madison, WI, USA) or AGAP2-pGL4.10 and 0.1 μg of pCH110 vector (Addgene, Cambrigde, MA, USA) as control for transfection efficiency. After 24 h of transfection, cells were serum starved for 12 h and then treated or not with 8 ng/ml TGFβ1. Luciferase and β-galactosidase activities were determined following manufacturer's instructions. Data analysis was performed as follows: the average value of the assay background was subtracted to each sample and luciferase activity values were normalised to β-Galactosidase activity values.

2.10 Animal model of hepatic fibrosis

The experimental protocol was approved and performed according to the guidelines of the Animal Care Committee of the University of Navarra. Eight-week-old male Sprague-Dawley rats (~250 g) were divided into two groups, including a control group (n=5) and an experiment group (n=5). Animals were housed in a 12:12 h light-dark cycle at an ambient temperature 22°C with food and water available *ad libitum*.

Thioacetamide (TAA) (Sigma-Aldrich) was administered to the experiment group in sweetened drinking water (sucrose solution 50 g/L) for 9 weeks at a concentration of 300 mg/L. Control animals were given vehicle alone. Animals were anesthetized using pentobarbital sodium (50 mg/Kg) and sacrificed by cervical dislocation. The liver was collected, washed in PBS and frozen in liquid nitrogen.

2.11 Protein extraction in animals

Liver tissue was lysed in RIPA buffer and homogenates were subjected to western blot analysis.

2.12 RNA extraction in animals

Total RNA from liver tissue was extracted using the automated Maxwell system from Promega (Madison, WI, USA). Reverse transcription was developed with Moloney murine leukemia virus reverse transcriptase (MMLV-T) (Invitrogen) in the presence of RNaseOUT (Invitrogen). Real-time PCR was performed using the iQ SYBR Green Supermix (Bio-Rad) in an iCycler (Bio-Rad). To monitor the specificity final PCR products were analyzed by melting curves and the amount of each transcript was expressed as the n-fold difference relative to the control gene H3 Histone Family Member 3A (H3F3A) ($2^{\Delta Ct}$, where ΔCt represents the difference in threshold cycle between the control and target genes).

Gene		Sequence
aSMA	Forward	5'-CCAGGGCTGTTTTCCCATCC-3'
	Reverse	5'-GTCATTTTCTCCCGGTTGGCC-3'
Col1a1	Forward	5'-CAGATTGAGAACATCCGCAG-3'
	Reverse	5'-TCGCTTCCATACTCGAACTG-3'
H3F3A	Forward	5'-AAAGCCGCTCGCAAGAGTGCG-3'
	Reverse	5'-ACTTGCCTCCTGCAAAGCAC-3'

2.13 Receptor trafficking

U2OS cells were seeded in 24-well plates at a density of 5 x 10^4 cells per well in 500 µl serum-free DMEM and transfected with scramble or AGAP2 siRNA with Lipofectamine RNAiMAX. The day following cell seeding, U2OS cells were transfected with the scramble or AGAP2 siRNA for the second time, and co-transfected with the TGFR2-SNAPtag vector using PEI 25 kDa at a 1:4 ratio (w/v) (DNA:PEI). 48 h after vector transfection, U2OS cells were labeled with 5 µM SNAP-cell Oregon Green substrate (New England Biolabs, Ipswich, MA, USA) for 30 min at 37°C. Cells were washed with serum-containing DMEM and incubated in NucBlue-containing fresh medium for 30 min

at 37°C following the manufacturer's instructions. Images of live trafficking of TGFβ receptor TGFR2 were taken after 8 ng/ml TGFβ1 treatment, employing a 40x objective of the Evos FL Cell Imaging system from ThermoFisher Scientific (Waltham, MA, USA). The receptor movement and fluorescence intensity were analysed using ImageJ software.

2.14 AGAP2 over-expression

LX-2 cells were seeded at density of $5x10^4$ per well in a 24-well plate with 1 ml of DMEM. At 60% confluency cells were transfected with an empty pCMV6 vector or with the pCMV6 vector carrying AGAP2 using PEI 25 kDa with a 1:4 DNA to PEI ratio (w/v). 0.5 µg of DNA were used per well and the transfection medium was replaced after 2 h by growth medium. AGAP2 levels, and its effect, were analysed 48 h after transfection.

2.15 Data analysis

Data were analysed using the non-parametrical Kruskal-Wallis test to determine differences between all independent groups. All statistical analyses were conducted using GraphPad Prism 5 software. When significant differences were obtained ($p < 0.05$), differences between two groups were tested using the Mann–Whitney U test. All the experiments were independently performed at least three times and conducted in triplicate. Data are expressed as mean ± standard deviation of the mean (SD).

3. Results

3.1 AGAP2 is involved in viability, proliferative rate and migration of LX-2 cells in response to TGFβ1

Activated hepatic stellate cells (HSC) are the main cells responsible for liver fibrogenesis, a process modulated by the pro-fibrogenic cytokine TGFβ1. The activated phenotype of HSC is characterised by a high rate of proliferation and migration. In order to investigate the potential role of AGAP2 in TGFβ1-mediated fibrogenesis in HSCs, the effects of AGAP2 knock-down in LX-2 cells treated with TGFβ1 were initially studied. This cell line of human immortalised HSC has been extensively employed in the study of fibrogenesis. LX-2 cells were transfected with scramble or AGAP2 siRNA and viability and proliferation were determined using a real-time cell analysis (RTCA) iCELLigence instrument (Fig. 1), as described in Material and Methods (Fig. 1A, upper left panel). Changes in cellular impedance were analysed in a label-free, real-time manner and expressed as cell index (CI). Impedance changes were monitored every hour for 90 h in scramble- and AGAP2-siRNA transfected LX-2 cells before and after TGFβ1 treatment. RTCA curves showed a rapid increase in CI in the first 5 h due to cell adhesion, and after this time point, the increase was slow down due to cell proliferation. AGAP2 silencing significantly prevented the TGFβ1-induced proliferation of LX-2 cells at the indicated time points (Fig. 1A, right panel). AGAP2 down-regulation affected the total number of LX-2 cells since the RTCA curve of AGAP2 silenced cells showed a remarked decrease of the CI values after 22 h with TGFβ1 (time-point of the assay: 70 h). Control cells were viable for 37 h after TGFβ1 addition (time-point of the assay: 85h) (Fig. 1A, lower left panel).

To further investigate the potential role of AGAP2 in HSC proliferation, real-time proliferation assays were performed using IncuCyte S3 Live-Cell Analysis System. LX-2 cells were transfected with scramble or AGAP2 siRNA and treated or not with TGFβ1. Cell proliferation was visualised and quantified every 4 h for 72 h with a 10x objective. As shown in Figure 1B, left panel, TGFβ1 significantly increased the proliferation of scramble siRNA-transfected LX-2 cells after 72 h of treatment compared to non-treated cells. However, AGAP2 siRNA transfection prevented the the increase in cell proliferation induced by TGFβ1. Time-course quantitative analysis showed that the proliferative effect of TGF β1 in control cells was significant at 24 h. After 48 h of stimulation with TGFβ1, scramble siRNA-transfected cells showed 80% confluence while the confluence of AGAP2-silenced cells was 40%. In contrast to scramble siRNA-transfected cells, which reached 100% confluence after 72 h with TGFβ1 treatment, AGAP2 down-regulated cells confluence was 65% at this time-point (Fig. 1B, right panel).

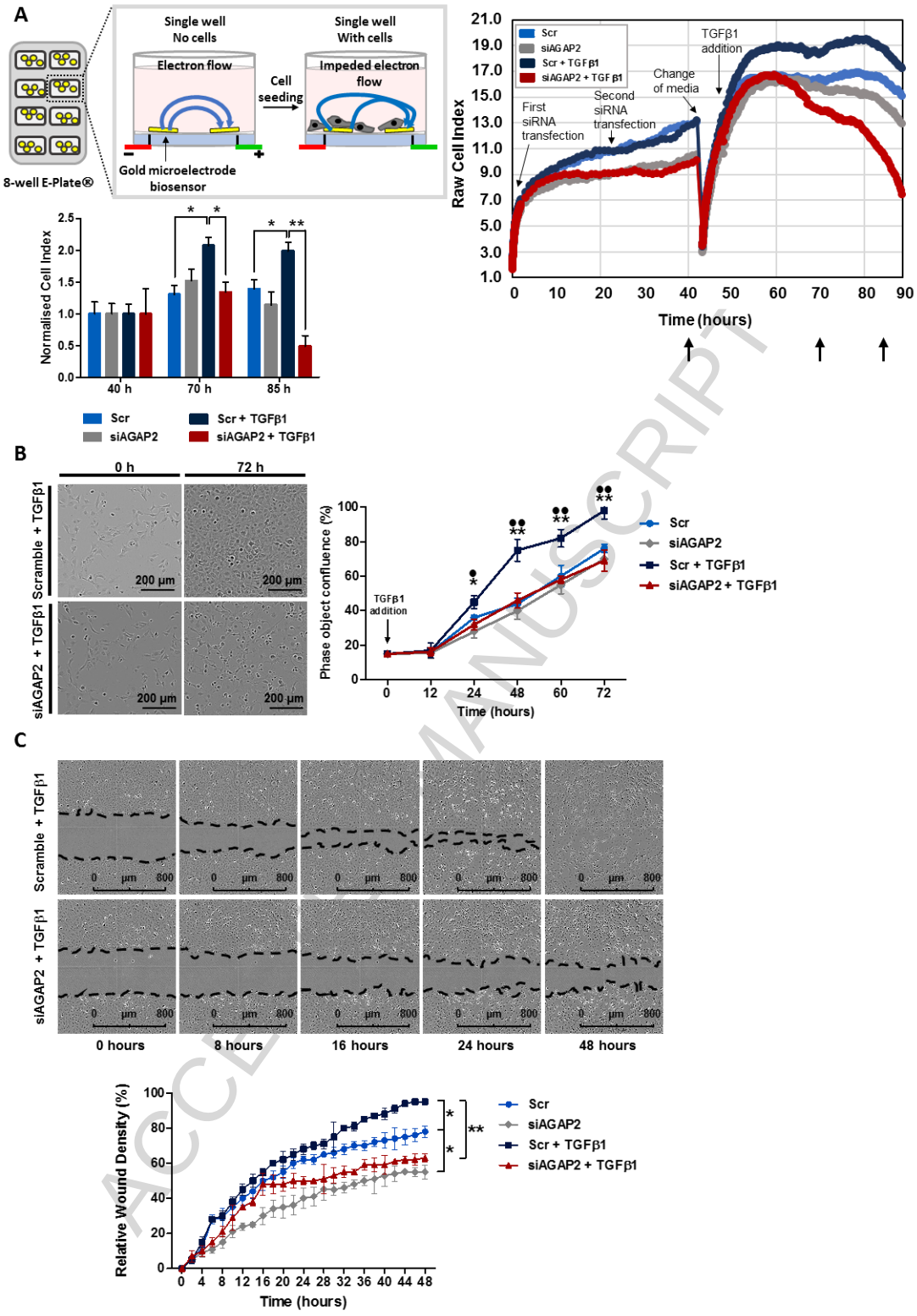

Figure 1. Analysis of AGAP2 in viability, proliferation and migration of LX-2 cells in response to TGFβ1. A) Cell viability assay in LX-2 cells using the real-time cell analysis (RTCA) iCELLigence instrument. Upper left panel: Overview of cellular impedance apparatus. Lower black arrow indicates the position of the gold microelectrode biosensors. Electron flow changes due to the presence of cells are represented with blue arrows. Changes in cell physiological properties that modulate the physical contact between cell and electrode are reflected by changes in the measured impedance, defined by a non-dimensional cell index (CI). Right panel: RTCA curves of LX-2 cells transfected with scramble siRNA (Scr) or AGAP2 siRNA (siAGAP2). After 48 h of transfection, LX-2 cells were treated with or without 8 ng/ml TGFβ1. Impedance

changes were monitored for 90 h. Lower left panel: Normalised CI values at different time-points of the assay: 40h, 70h and 85h. Lower black arrows indicate the analysed time-points represented in the lower left panel. **B)** Real-time proliferation assay in LX-2 cells using IncuCyte S3 Live-Cell Analysis System. LX-2 cells were transfected with scramble siRNA (Scr) or AGAP2 siRNA (siAGAP2) and treated with or without 8 ng/ml TGFβ1. Cell proliferation was visualised (left panel) and quantified (right panel) every 4 h for 72 h using a 10x objective. Scale bar 200 µm. **C)** Real-time wound-healing assay in LX-2 cells using IncuCyte S3 Live-Cell Analysis System. LX-2 cells were transfected with scramble siRNA (Scr) or AGAP2 siRNA (siAGAP2), pre-treated with mitomycin for 2 h and treated with or without 8 ng/ml TGFβ1. Scratch wound-healings were monitored every 2 h for 48 h using a 4x objective. Data from A, B and C are expressed as the mean ± SD of three independent experiments. Real-time viability assay: *p<0.05. Real-time proliferation assay: *p<0.05 and **p<0.005 for Scr+TGFβ1 *vs* Scr; •p<0.05 and ••p<0.005 for Scr+TGFβ1 *vs* siAGAP2+TGFβ1.

As activated HSC acquire migratory properties, the potential implication of AGAP2 in this parameter was investigated. LX-2 cells were transfected with either scramble siRNA or AGAP2 siRNA and then, pre-treated with 10 µM mitomycin for 2 h to inhibit cell proliferation before TGFβ1 addition. After TGFβ1 treatment transfected cells were monitored every 2 h for 48 h using IncuCyte S3 Live-Cell Analysis System (4x objective) (Fig. 1C). Quantitative analysis of scratch wound-healing showed significant differences in the migratory response to TGFβ1 of LX-2 cells transfected with AGAP2 siRNA at the end of the experiment. Over the course of 48 h, the wounds were completely closed in cells transfected with scramble siRNA and treated with TGFβ1 (Fig. 1C). However, a significant prevention in TGFβ1-induced migration of LX-2 cell was observed under the effect of AGAP2 siRNA compared to scramble siRNA transfected cells (Fig. 1C).

3.2 TGFβ1-induced changes on pro-fibrogenic gene expression in LX-2 cells are modulated by AGAP2

Next, the role played by AGAP2 on the profibrogenic transcriptional profile induced by TGFβ1 in LX-2 cells was investigated. A RT^2 Profiler PCR Array focused on 84 genes involved in human fibrosis was employed. Relative expression of fibrotic genes in LX-2 cells transfected with scramble siRNA, LX-2 cells transfected with scramble siRNA treated with TGFβ1 and AGAP2 silenced LX-2 cells treated with TGFβ1, were analysed and the resulting heat maps can be observed in Supplementary Figure 1S.

Initially, those genes significantly upregulated or downregulated by TGFβ1 in scramble-transfected LX-2 cells (genes falling outside the central area in Fig. 2A) were identified. In order to address if the expression of these genes depended on AGAP2, TGFβ1-mediated gene expression in scramble siRNA-transfected cells was compared to TGFβ1-mediated gene expression in AGAP2 knocked-down cells. As suspected, it was confirmed that AGAP2 silencing, partially prevented TGFβ1-mediated gene expression at the mRNA level (see clustergram in Fig. 2B).

Interestingly, the identified genes included matrix metalloproteinases (*MMP1*, *MMP3*, *MMP9*), interleukins (*IL1A*), C-X-C motif chemokine receptor 4 (*CXCR4*), as well as

collagens (*COL1A2*), endothelins (*EDN1*), lysil oxidases (*LOX*), actins (*ACTA2,* smooth muscle α-2 actin), inhibit beta E subunit (*INHBE*), platelet derived growth factor subunit B (*PDGFB*) and transforming growth factor beta 2 (*TGFB1*), (Fig. 2C, D).

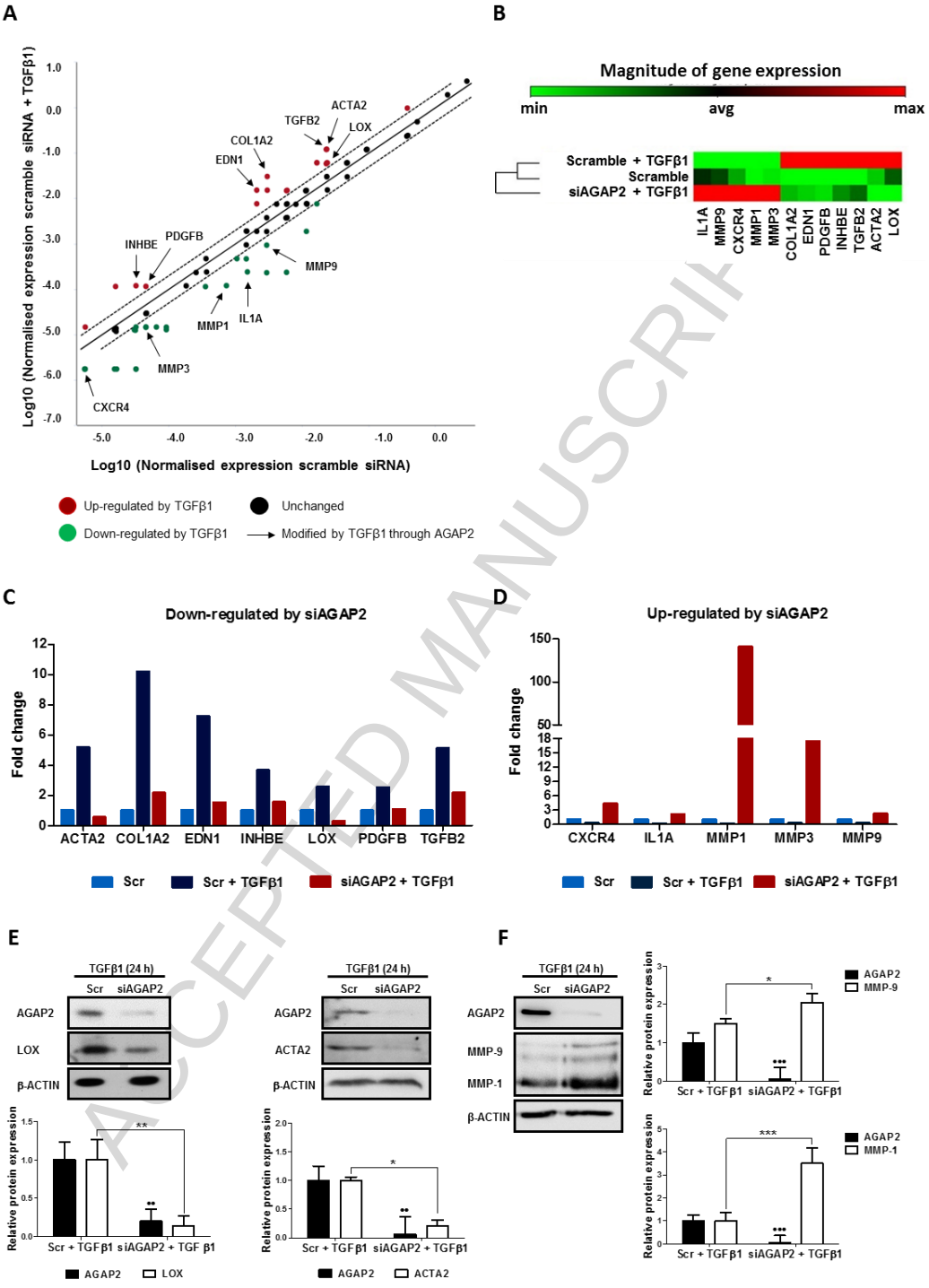

Figure 2. Profibrogenic transcriptional profile of LX-2 cells in response to TGFβ1 and in the presence/absence of AGAP2 using RT2 Profiler PCR array. Cells were transfected with scramble siRNA (Scr) or AGAP2 siRNA (siAGAP2) and treated with or without 8 ng/ml TGFβ1 for 24 h. Comparisons among groups were analysed and values were normalised to mRNAs of ACTB, B2M, GAPDH and RPLP0. A) Scatter-plot comparing Scr vs TGFβ1-treated Scr LX-2 cells and showing the normalised expression of the 84 genes in the array. Red colour: normalised expression of genes up-regulated by TGFβ1. Green colour: normalised expression of genes down-regulated by TGFβ1. Black colour: normalised expression of unchanged genes. Arrows indicate genes modified by TGFβ1 through AGAP2. B) Clustergram comparing the three

groups and showing the genes modified by TGFβ1 through AGAP2. C) Fold change of genes down-regulated by siAGAP2. D) Fold change of genes up-regulated by siAGAP2. E). Validation of LOX and ACTA2 (smooth muscle α-2 actin) protein expression using western-blot (upper panel, representative immunoblots). F) Validation of MMP1 and MMP9 protein expression using western-blot (upper panel, representative immunoblots). β-actin protein levels were used as a loading control for total protein. Data from the array were analysed once (using 800 ng of RNA per well) and protein validation of the data (Figures 2E and 2F) are expressed as the mean ± SD of two independent experiments. *p<0.05; **p<0.005.

To validate some of these findings at the protein level, western-blots were performed. We were able to demonstrate for the first time that TGFβ1-mediated overexpression of lysil oxidase and smooth muscle α-2 actin are dependent on AGAP2 expression (Fig. 2E), as its suppression significantly prevents their TGFβ1-mediated increase. Protein levels of metalloproteinases 1 and 9 were also significantly altered in AGAP2 knocked-down cells, confirming that AGAP2 silencing attenuates some effects of TGFβ1 in LX-2, (Fig 2F).

3.3 AGAP2 expression is enhanced by TGFβ1 treatment

The possible role of TGFβ1 in the regulation of *AGAP2* gene expression and protein levels was explored. A luciferase reporter assay was performed in order to assess the transcriptional rate of the *AGAP2* promoter. LX-2 cells were transfected with the promoter-less luciferase pGL4.10 vector or with a pGL4.10 vector carrying a fragment of ~1000 bp upstream the transcription start site for *AGAP2* (*AGAP2*-luc). Then, cells were treated with TGFβ1 for 6, 12 and 24 h. As shown in Fig. 3A, *AGAP2*-luc transfected cells treated with TGFβ1 for 6 h presented a significantly higher luciferase activity than the non-treated cells. Interestingly, TGFβ1 induced a transient promoter activation as the reporter activity returned to basal levels 12 h after TGFβ1 treatment and remained at those basal levels 24 h after TGFβ1 treatment (Supplementary Fig. 2S).

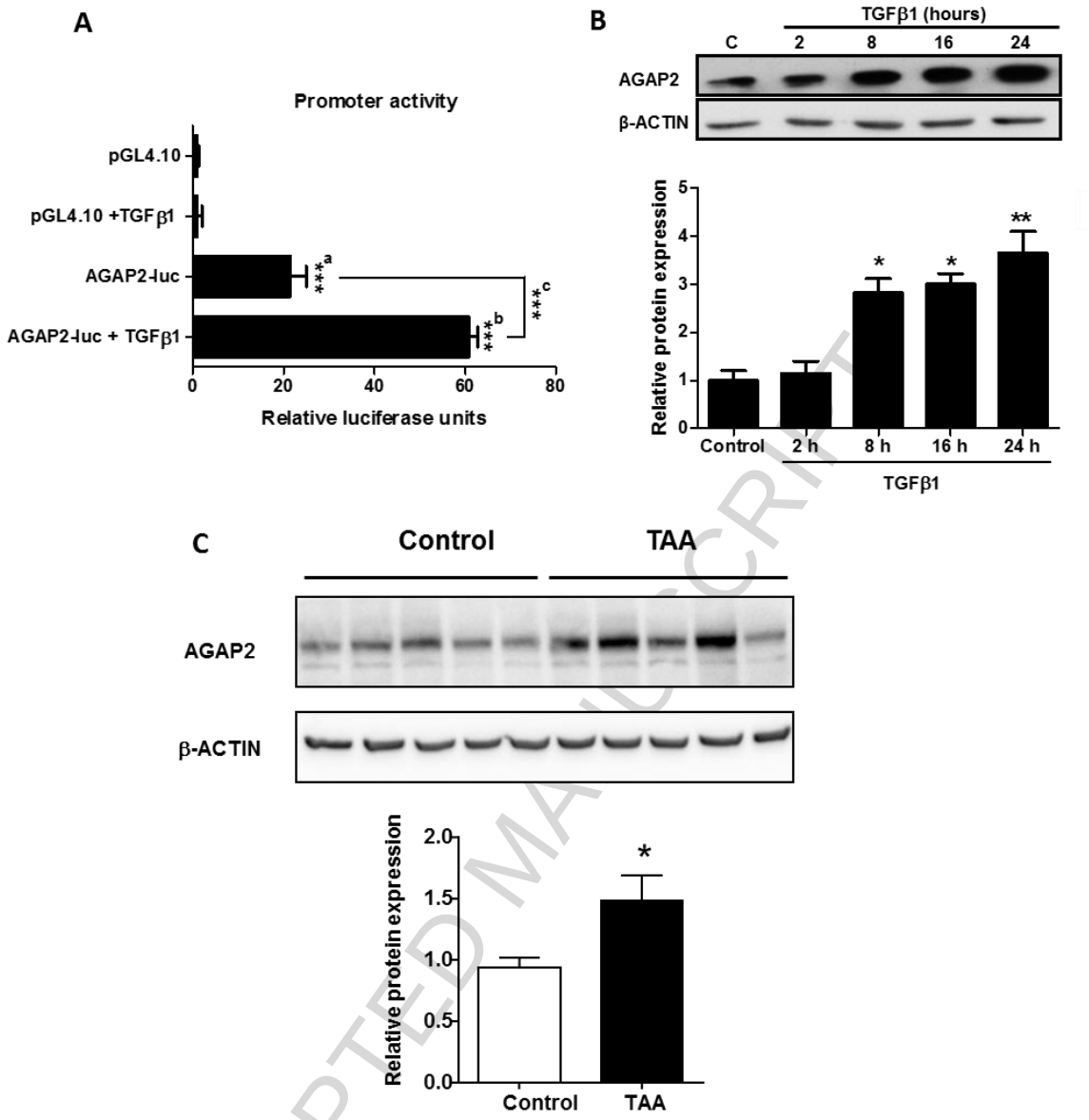

Figure 3. Expression of AGAP2 in LX-2 cells in response to TGFβ1 and in an animal model of fibrotic liver diseases. A) Luciferase reporter assay. LX-2 cells were transfected with (promoter-less) luciferase pGL4.10 vector or with a pGL4.10 vector carrying a fragment of ~1000 bp upstream the transcription start site for AGAP2 (AGAP2-luc). TGFβ1 was added into the cells for 6 h. B) Protein expression levels of AGAP2 in LX-2 cells treated with 8 ng/ml TGFβ1 for the indicated time points were quantified by western blot. β-actin protein levels were used as a loading control for total protein. A representative immunoblot is shown. C) Protein expression levels of AGAP2 were quantified by western blot in a thioacetamide-induced animal model of fibrotic liver disease. β-actin protein levels were used as a loading control for total protein. A representative immunoblot is shown. Data from *in vitro* experiments A and B are expressed as the mean ± SD of three independent experiments. Figure A ***p<0.0005 for (a) AGAP2-luc *vs* pGL4.10, (b) AGAP2-luc+TGFβ1 *vs* pGL4.10 + TGFβ1, (c) AGAP2-luc+TGFβ1 *vs* AGAP2-luc 1023/+36. Figure B *p<0.05 and **p<0.005 for TGFβ1 *vs* control. Figure C *p<0.05 TAA *vs* control.

AGAP2 protein levels in LX-2 cells and in the rat HSC cell-line CFSC-2G were also analysed by western-blot after TGFβ1 stimulation at different time points. TGFβ1 induced a significant increase in AGAP2 levels in a time-dependent manner as shown here at 8, 16 and 24 h post-treatment (Fig. 3B and Supplementary Fig. 3S).

To validate these results in a pathophysiological context, protein levels of AGAP2 in liver samples obtained from rats which presented a high degree of hepatic fibrosis were analysed. This model is based in the treatment of rats with thioacetamide (TAA) for 9 weeks (see Materials and Methods). As expected, TAA-cirrhotic rats presented significant increased levels of molecular markers of fibrosis evaluated by qPCR (Supplementary Figure 4S). Western-blot analysis of liver samples from 5 TAA-cirrhotic rats as well as from control rats, showed a significant increase in the expression of AGAP2 in the TAA-cirrhotic rats (Fig. 3 C).

3.4 AGAP2 plays a role in TGFβ receptor type II trafficking

Recent reports have suggested that AGAP2 is involved in endosomal trafficking promoting the fast recycling of receptors [6]. In addition, AGAP2 is known to regulate the retrograde transport between early endosomes and trans-Golgi network by interacting with AP-1 [21]. Interaction of AGAP2 with AP-1 as well as its involvement in receptor recycling suggest that AGAP2 might play a role in TGFβ1 receptor type II (TGFR2) signalling and trafficking. To evaluate this possibility, a TGFR2-SNAPtag construct was prepared and transfected into U2OS cells as a model to visualise the movements and distribution of TGFR2.

In cells transfected with scramble siRNA, most of the TGFR2 detected was concentrated in vesicles around the nucleus (Fig. 4A).

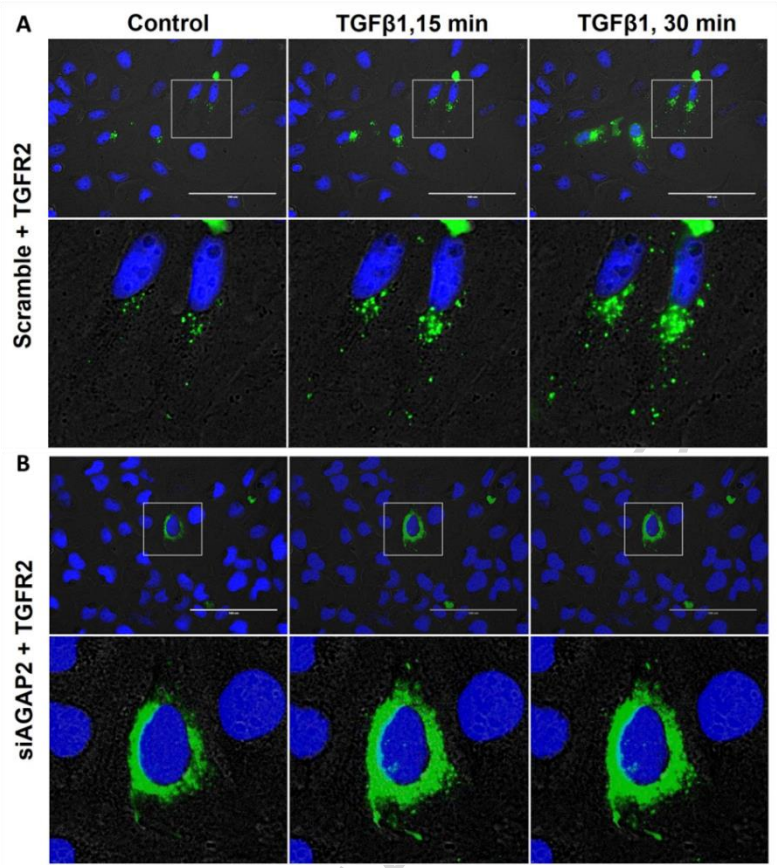

Figure 4. Live tracking of TGFR2-trafficking in U2OS cell line using SNAP-tag technology. U2OS cells were co-transfected with Scramble or AGAP2 siRNA (siAGAP2) and TGFR2-SNAPtag construct. Cells were incubated with 5 µM SNAP-Cell Oregon Green substrate and NucBue Live ReadyProbes Reagent for 30 and 20 min, respectively. Fluorescence images of localisation of the TGFR2-SNAPtag were taken before TGFβ1 stimulation and after 15 and 30 min of 8 ng/ml TGFβ1 treatment using a 40x objective. A) TGFR2 signal in scramble siRNA-transfected U2OS cells. B) TGFR2 signal in AGAP2 siRNA-transfected U2OS cells. Green colour: TGFR2-SNAPtag labelled with the SNAP-Cell Oregon Green photostable green fluorescent substrate. Blue colour: Nuclei stained with NucBue Live ReadyProbes Reagent. Representative image of six independent experiments. Scale bar 100 µm.

Stimulation with 8 ng/ml TGFβ1 resulted in the movement of TGFR2, which was distributed on punctate structures throughout the cytoplasm (Fig. 4A, TGFβ1, 15 min and 30 min). Indeed, though TGFR2 was still found in the perinuclear region, 30 min after treatment a wider distribution of the receptor around the cell was clear with some TGFR2 detected near the cell periphery (Fig. 4A and Supplementary Fig. 5SA). However, in U2OS cells transfected with siAGAP2, TGFR2 was mainly detected in the perinuclear region even after 30 min of TGFβ1 stimulation (Fig. 4B and Supplementary. Fig. 5SA). Similar results were obtained in LX-2 cells treated in the same conditions (Supplementary Fig. 5SB). This observation strongly suggests that AGAP2-silencing results in the disruption of the normal TGFR2 trafficking process.

3.5 AGAP2 is involved in the effect of TGFβ1 on LX-2 collagen type I protein levels

The fact that AGAP2 alters TGFβ receptor II trafficking within the cell could explain why it mediates some of the TGFβ1-induced gene expression changes. One of those genes, detected in the PCR array (Fig. 2), was collagen, and one of the key features of activated HSC is the increased production of collagen type I. To study the possible role of AGAP2 in LX-2 collagen expression, the correlation between collagen type I and AGAP2 levels on LX-2 cells in response to TGFβ1 treatment was analysed. Western-blot analysis of protein levels of procollagen α1(I) and AGAP2 was carried out in LX-2 cells treated with TGFβ1 at different time points, from 2 to 48 h. As shown in Fig. 5A, TGFβ1 treatment caused an enhancement of both collagen type I and AGAP2 levels, with maximum levels at 24 h of TGFβ1 treatment.

To determine whether the effect of TGFβ1 on collagen type I protein levels depended on AGAP2 expression, we analysed protein levels of collagen type I in response to this cytokine either in AGAP2 knocked-down LX-2 cells or in LX-2 cells with an over-expression of AGAP2. Silencing of AGAP2 was carried out as described before by transfection with siAGAP2, and procollagen α1(I) levels were analysed after 24 h of treatment with TGFβ1.

AGAP2 knocked-down cells treated with TGFβ1 presented lower levels of collagen type I compared to control cells also treated with TGFβ1 (Fig. 5B).

Similar experiments were carried out in LX-2 with an over-expression of AGAP2, which was obtained by transfection with a pCMV6 vector containing AGAP2, as described in Materials and Methods. Collagen type I levels were significantly enhanced by AGAP2 over-expression in LX-2 cells both, with and without TGFβ1 treatment (Fig. 5C). These results suggest that AGAP2 contributes to the effect of TGFβ1 on collagen type I protein levels in HSC.

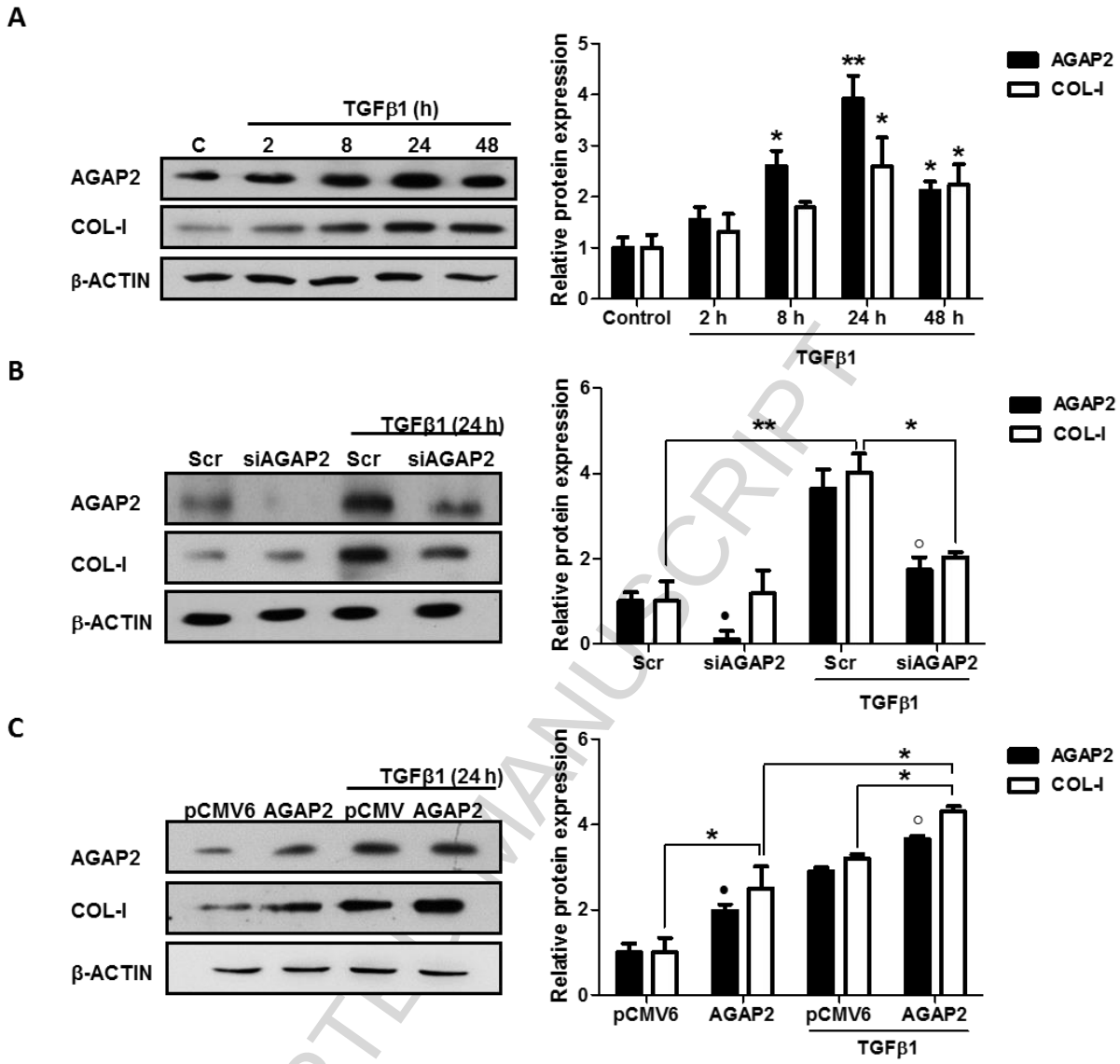

Figure 5. Effect of AGAP2 on TGFβ1-induced collagen type I levels in LX-2 cells. A) Collagen type I (COL-I) protein levels determined by western-blot in LX-2 cells treated with 8 ng/ml TGFβ1 for the indicated time points. B) Protein levels of AGAP2 and COL-I determined by western-blot in LX-2 cells transfected with scramble siRNA (Scr) or with AGAP2 siRNA (siAGAP2) for 48 h and treated with 8 ng/ml TGFβ1 for 24 h. C) Protein levels of AGAP2 and COL-I determined by western-blot in LX-2 cells transfected with pCMV6-empty vector (pCMV6) or with pCMV6-AGAP2 (AGAP2) for 48 h and treated with 8 ng/ml TGFβ1 for 24 h. A-C) β-actin protein levels were used as a loading control for total protein. Representative immunoblots are shown. Data from Figure 5A are expressed as the mean ± SD of four independent experiments. Data from Figure 5B and 5C are expressed as the mean ± SD of three independent experiments *p<0.05 and **p<0.005.

3.6 FAK is involved on the effects of TGFβ1 in collagen mediated by AGAP2

The molecular mechanisms involved in the regulator role of AGAP2 on the effect of TGFβ1 on collagen type I production by HSC were studied. We had previously shown that collagen levels of HSC could be enhanced by p38 MAPK [22] and Smads [23] in response to different stimuli, like TGFβ1 [24] and ER stress [25]. It has also been

described that TGFβ1 stimulates FAK synthesis through a Smad and p38 dependent mechanism, and that FAK phosphorylation levels are directly related to FAK induced expression [26].

Previous reports indicate that AGAP2 binds to and regulates FAK, acting as a regulator of integrin adhesion complexes [3]. We hypothesised that TGFβ1 might increase collagen type I in LX-2 cells through AGAP2-activated FAK. First, relative phospho-FAK *versus* total-FAK levels in LX-2 cells treated with TGFβ1 for different times were analysed (Fig. 6A). Western-blot detection showed that FAK phosphorylation levels were significantly higher 24 h following TGFβ1 addition. To investigate if phospho-FAK levels depended on AGAP2 expression, the effects of AGAP2 knock-down and AGAP2 over-expression in phospho-FAK protein levels were studied. AGAP2 siRNA significantly prevented the increase of phospho-FAK compared to LX-2 cells transfected with scramble siRNA (Fig. 6B, upper panel). Consistent with this result, cells overexpressing AGAP2 showed a significant increase in phospho-FAK levels compared to control cells transfected with empty vector (Fig. 6B, lower panel). To elucidate the role played by FAK in collagen type I protein expression induced by TGFβ1 through AGAP2, LX-2 cells were transfected with AGAP2 or empty vector for 48 h, pre-treated with a chemical inhibitor of FAK (PF-573228) and then treated with TGFβ1. The levels of collagen type I after TGFβ1 were not altered by FAK inhibitor in cells transfected with empty vector. However, FAK inhibitor prevented the increase of collagen type I protein levels caused by TGFβ1 in LX-2 cells transfected with AGAP2 plasmid (Fig. 6C, left panel). Similar experiments were carried out with PD98059, an inhibitor of MEK1 and therefore of ERK (extracellular-signal-regulated kinase), a kinase that has been described as a downstream target of FAK [27]. ERK inhibition was also effective in preventing the effect of TGFβ1 on collagen type I levels in LX-2 with an over-expression of AGAP2 (Fig. 6C, right panel).

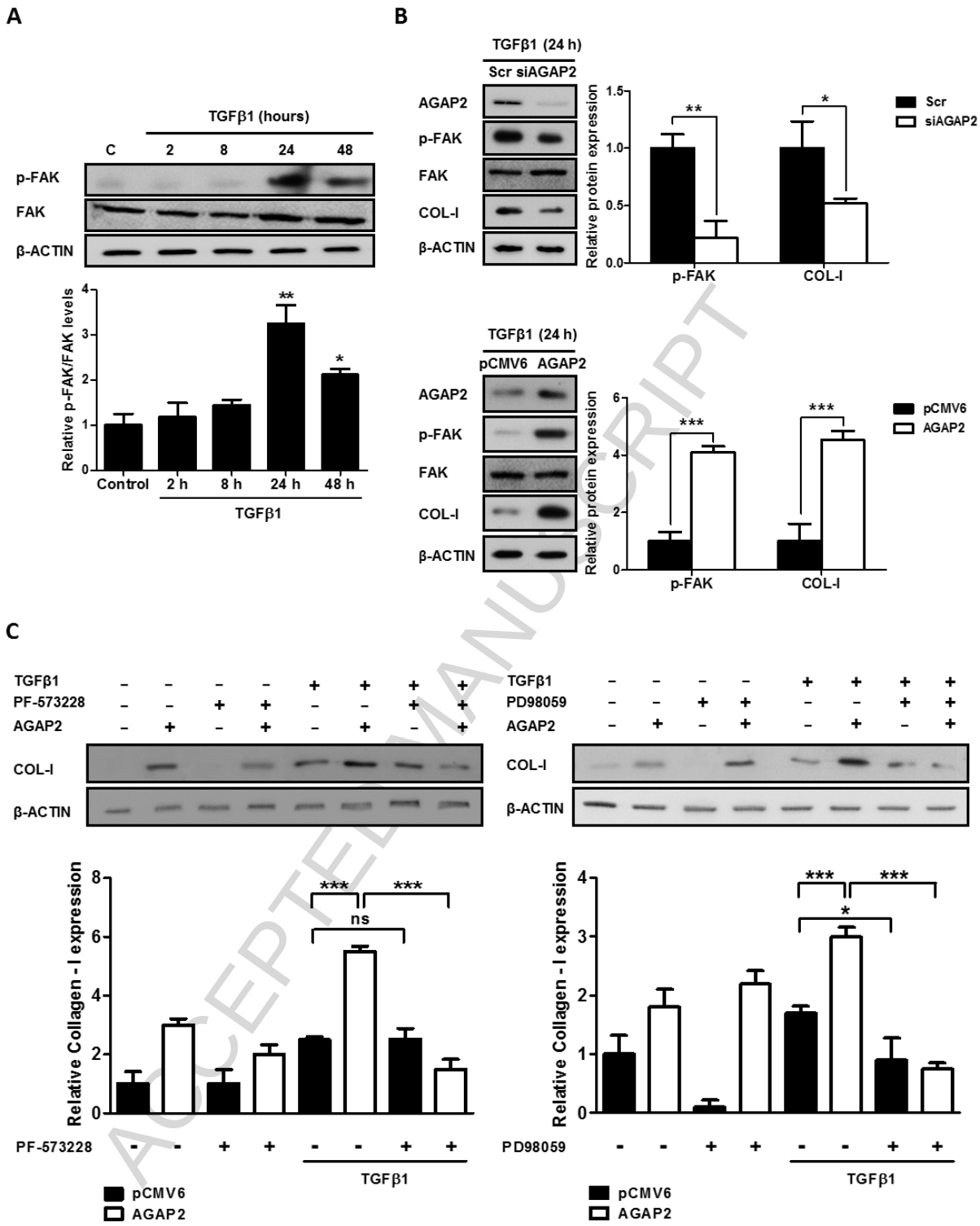

Figure 6. Molecular mechanism involved in the mediator role of AGAP2 on the pro-fibrogenic effects of TGFβ1 in LX-2 cells. A) Relative protein levels of phospho-FAK (p-FAK) *versus* total-FAK determined by western-blot experiments in LX-2 cells treated with 8 ng/ml TGFβ1 for the indicated time points B) Collagen type I (COL-I) and relative p-FAK versus total-FAK protein levels were determined by western-blot in LX-2 cells transfected with scramble siRNA (Scr) or with AGAP2 siRNA (siAGAP2) (upper panel); or transfected with pCMV6-empty vector (pCMV6) or with pCMV6-AGAP2 vector (AGAP2) (lower panel) for 48 h. 8 ng/ml TGFβ1 was added into the cells for 24 h in all cases. C) Protein levels of COL-I were determined by western-blot in LX-2 cells transfected with pCMV6-empty vector (pCMV6) or pCMV6-AGAP2 vector (AGAP2) for 48 h. LX-2 cells were pre-treated with PF-573228 (a FAK inhibitor) (left panel), or with PD98059 (MEK 1/ERK

inhibitor) (right panel) for 30 min and treated or not with 8 ng/ml TGFβ1 for 24 h. β-actin protein levels were used as a loading control for total protein. Representative immunoblots are shown. Data are expressed as the mean ± SD of three independent experiments. . *p<0.05, **p<0.005 and ***p<0.0005; (a) vs pCMV6, (b) vs AGAP2, (c) vs pCMV6 + TGFβ1, (d) vs pCMV6 + PF-573228 or pCMV6 + PD98059, (e) vs AGAP2 + TGFβ1.

4. Discussion

Liver fibrosis is a pathological condition caused by persistent liver damage and characterised by an excessive accumulation of extracellular matrix (ECM) proteins mainly produced by activated hepatic stellate cells (HSC). Many different agents, including oxidative stress, inflammatory and immunological factors and cytokines, have been shown to be regulators of the biology of HSC and therefore to have a role as liver fibrosis modulators. Among them, TGFβ1 presents a key role as a pro-fibrogenic factor, acting on HSC, and affecting parameters like epithelial-mesenchymal transition (EMT), collagen, alpha-smooth muscle actin (α-SMA) and fibronectin production and remodelling of ECM. To investigate the possible role played by AGAP2 in the response of HSC to TGFβ1 several parameters were analysed, such as proliferation, migration, as well as the fibrogenic gene expression of AGAP2-silenced HSC treated with TGFβ1. We found changes in all these processes: migration and proliferation in response to TGFβ1 were significantly delayed in HSC in which AGAP2 expression was down regulated (Fig. 1); and the gene expression profile comparison revealed that AGAP2 is required for TGFβ1-induced expression of some fibrogenic genes (including collagen, α-SMA and lysyl oxidase) and TGFβ1-mediated reduction of some anti-fibrogenic genes (including MMP-1 and MMP-9) in HSC (Fig. 2). Therefore, our results suggest that the response to TGFβ1 in HSC is in some extent modulated by AGAP2.

It is well established that AGAP2 interacts with and enhances AKT activity [2]. And it has also been described that blocking PI3K signalling (and therefore AKT activation) leads to reduced extracellular matrix deposition in HSCs [28]. Furthermore, down-regulation of collagen and up-regulation of MMP-1 have been linked to inactivation of AKT in dermal fibroblasts [29] whilst in cardiac fibroblasts, TGFβ1-induced lysyl oxidase expression required activation of the PI3K/AKT pathway [30]. Therefore, it could be that AGAP2-mediation of TGFβ1-induced changes in HSCs is achieved through sustainment of AKT signalling.

Interestingly, we found that TGFβ1 was a regulator of AGAP2 expression, since both the activity of the *AGAP2* promoter as well as AGAP2 protein levels were enhanced by treatment with TGFβ1 (Fig. 3), pointing to an autocrine response that has already been

described for TGFβ1 in other models [31]. As TGFβ1 delayed proliferative response (24 to 72 h in our hands, Fig. 1B) depends on AKT signalling according to the literature [32], it is possible that the increased levels of AGAP2 after TGFβ1 treatment (as early as 8 h post treatment, Fig.3B) contributed to an enhancement of AKT signalling that would be responsible for some of the changes observed. However, the role of AGAP2 in mediating the response to TGFβ1 could also be due to other mechanisms. AGAP2 is a member of ArfGAP family proteins (Arf GTPase activating proteins) which are involved in receptor trafficking and recycling, as well as in integrin activation and signalling [5]. TGFβ1 binds to two different receptors TGFRI and II, which are internalised and should be recycled for an optimum response to the cytokine. We found that the recycling of TGFRII back to the membrane was altered by AGAP2 silencing (Fig. 4) similar to what has been observed for the β2-adrenergic receptor [8]. TGFRII mobilisation occurred within 30 min of TGFβ1 treatment, conditions under which AGAP2 levels are not yet affected by TGFβ1 administration (Fig. 3B). These results suggest that AGAP2 may be involved in potentiating the effects of TGFβ1 in HSC through the recycling of its receptor to the membrane.

Collagen I is the main component of the fibrotic liver and its regulation by different factors such as TGFβ1 has been extensively studied. We found a correlation between collagen and AGAP2 levels in HSC treated with TGFβ1, since both proteins were enhanced by TGFβ1-treatment, and depleted or increased expression of AGAP2 correlated with diminished or enhanced collagen type I levels in response to TGFβ1, suggesting a positive relationship between them (Fig. 5).

FAK is a cytosolic protein kinase recruited to focal adhesion (FA) after clustering of integrins and then activated in an adhesion-mediated process between integrins and ECM proteins [33]. Previous reports had shown a pivotal role for FAK in regulating liver fibrosis. The disassembly of FA complexes in HSCs prevents hepatic fibrosis in animal models [34] and abolishment of FAK activation blocks α-SMA and collagen expression, and inhibits the formation of stress fibres in TGF-β1-treated HSCs [35]. Interestingly, AGAP2 has been shown to interact directly with FAK [3], pointing to this kinase as a potential target of AGAP2. We found that altering AGAP2 levels, either by blocking or enhancing them, had an inhibitory or activating effect on FAK, respectively. These changes also correlated with changes in collagen type 1 levels. The sustained high levels of fibrogenic proteins in response to TGFβ1 could be a result of a cross-talk mechanism between TGFβ1 and adhesion-dependent signalling pathways. The use of specific

inhibitors for FAK and MEK1 (the activator kinase of ERK, a target of FAK [27]) confirmed the mediator role of these kinases in the profibrogenic action of TGFβ1 and AGAP2.

4.1 **Conclusions**

In summary, we found that AGAP2 is a regulator of HSC through modulating some of key effects induced by TGFβ1 such as proliferation, migration, as well as gene expression of some pro-fibrogenic genes. The work also demonstrates that the expression of AGAP2 itself is also modulated by TGFβ1. Moreover, the results obtained reveal that AGAP2 is involved in TGFβ1-induced increase of collagen type I protein levels in LX-2 cells, a process that is mediated at least in part, through the AGAP2-induced activation of FAK. In addition, AGAP2 could be playing a role in the TGFβ receptor type II trafficking. As a result, AGAP2 seems to be involved in TGFβ1 signaling that could contribute to the progression of hepatic fibrosis, suggesting AGAP2 as a potential new molecular target for liver fibrogenesis.

5. Bibliography

[1] T. R. Jackson, B. G. Kearns, and A. B. Theibert (2000) Cytohesins and centaurins: Mediators of PI 3-kinase-regulated Arf signaling. Trends in Biochemical Sciences 25:489-95.

doi: 10.1016/S0968-0004(00)01644-3

[2] C. B. Chan, K. Ye, C. B. Chan, and K. Ye (2007) PIKE GTPase are phosphoinositide-3-kinase enhancers, suppressing programmed cell death. J. Cell. Mol. Med. 11:39–53.

doi: 10.1111/j.1582-4934.2007.00014.x

[3] T. Vitali, S. Girald-Berlingeri, P. A. Randazzo, and P.W. Chen (2017) Arf GAPs: A family of proteins with disparate functions that converge on a common structure, the integrin adhesion complex. Small GTPases. 31:1-9.

doi: 10.1080/21541248.2017.1299271

[4] Y. Zhu, Y. Wu, J. I. Kim, Z. Wang, Y. Daaka, and Z. Nie (2009) Arf GTPase-activating Protein AGAP2 Regulates Focal Adhesion Kinase Activity and Focal Adhesion Remodeling. J. Biol. Chem. 284:13489–13496.

doi: 10.1074/jbc.M900469200

[5] Y. Shiba, W. Römer, G. A. Mardones, P. V Burgos, C. Lamaze, and L. Johannes (2010) AGAP2 regulates retrograde transport between early endosomes and the TGN. J. Cell Sci.123:2381–90.

doi: 10.1242/jcs.057778

[6] Y. Wu, Y. Zhao, X. Ma, Y. Zhu, J. Patel, and Z. Nie (2013) The Arf GAP AGAP2

interacts with β-arrestin2 and regulates β 2 -adrenergic receptor recycling and ERK activation. Biochem. J. 452(3):411–421.

doi:10.1042/BJ20121004

[7] Q. Qi, S. Kang, S. Zhang, C. Pham, H. Fu, D.J. Brat, and K.Ye (2017) Co-amplification of phosphoinositide 3-kinase enhancer A and cyclin-dependent kinase 4 triggers glioblastoma progression. Oncogene. 36(32):4562–4572.

doi: 10.1038/onc.2017.67

[8] X. Liu, Y. Hu, C. Hao, S. A. Rempel, and K. Ye (2007) PIKE-A is a proto-oncogene promoting cell growth, transformation and invasion. Oncogene. 26(34):4918–4927.

doi.org/10.1038/sj.onc.1210290

[9] J.Y. Ahn, Y. Hu, T. G. Kroll, P. Allard, and K. Ye (2004) PIKE-A is amplified in human cancers and prevents apoptosis by up-regulating Akt Proc. Natl. Acad. Sci. 101(18):6993–6998.

doi: 10.1073/pnas.0400921101

[10] X. Tang, Y. Feng, and K. Ye (2007) Src-family tyrosine kinase fyn phosphorylates phosphatidylinositol 3-kinase enhancer-activating Akt, preventing its apoptotic cleavage and promoting cell survival. Cell Death Differ.14(2):368–377.

doi: 10.1038/sj.cdd.4402011

[11] Y.S. Lim and W. R. Kim (2008) The Global Impact of Hepatic Fibrosis and End-Stage Liver Disease. Clin. Liver Dis.12(4):733–746.

doi: 10.1016/j.cld.2008.07.007

[12] S. L. Friedman (2008) Hepatic stellate cells: protean, multifunctional, and enigmatic cells of the liver. Physiol. Rev. 88(1):125–72.

doi: 10.1152/physrev.00013.2007

[13] E. Novo, L. Valfrè di Bonzo, S. Cannito, S. Colombatto, and M. Parola (2009) Hepatic myofibroblasts: A heterogeneous population of multifunctional cells in liver fibrogenesis. Int. J. Biochem. Cell Biol. 41(11):2089–2093.

doi: 10.1016/j.biocel.2009.03.010

[14] S. Robert, T. Gicquel, A. Bodin, V. Lagente, and E. Boichot (2016) Characterization of the MMP/TIMP Imbalance and Collagen Production Induced by IL-1β or TNF-α Release from Human Hepatic Stellate Cells PLoS One. 11 (4):e0153118.

doi: 10.1371/journal.pone.0153118

[15] S. Robert, T. Gicquel, T. Victoni, S. Valença, E. Barreto, B. Bailly-Maître, E. Boichot, and V. Lagente (2016) Involvement of matrix metalloproteinases (MMPs) and inflammasome pathway in molecular mechanisms of fibrosis. Biosci. Rep. 36(4):e00360.

doi:10.1042/BSR20160107

[16] I. Fabregat, J. Moreno-Càceres, A Sánchez, S Dooley, B Dewidar, G Giannelli, P. Ten Dijke, IT-LIVER Consortium (2016) TGF-β signalling and liver disease. FEBS J. 283(12):2219–2232.

doi:10.1111/febs.13665

[17] F. Huang and Y.G. Chen (2012) Regulation of TGF-b receptor activity. Cell Biosci. 2:9.

doi: 10.1186/2045-3701-2-9

[18] K. J. Livak and T. D. Schmittgen (2001) Analysis of Relative Gene Expression Data Using Real-Time Quantitative PCR and the 2(-Delta Delta C(T)) Method. METHODS. 25:402–408.

doi: 10.1006/meth.2001.1262

[19] Y. Doush, A.A. Surani, A. Navarro-Corcuera, S. McArdle, E. E. Billett, and C. Montiel-Duarte. Scientific Reports, *in press.*

doi: 10.1038/s41598-018-36888-x

[20] J.L. Wrana, L. Attisano, J. Cárcamo, A. Zentella, J. Doody, M. Laiho, X.F. Wang, and J. Massagué (1992) TGF beta signals through a heteromeric protein kinase receptor complex. Cell. 71 (6):1003–14.

doi: 10.1016/0092-8674(92)90395-S

[21] Z. Nie, J. Fei, R.T. Premont, and P.A. Randazzo (20015) The Arf GAPs AGAP1 and AGAP2 distinguish between the adaptor protein complexes AP-1 and AP-3. J. Cell Sci. 118: 3555–3566.

doi: 10.1242/jcs.02486

[22] M. Varela-Rey, C. Montiel-Duarte, J.A. Osés-Prieto, M.J. López-Zabalza, J.P. Jaffrèzou, M. Rojkind, and M.I. Iraburu (2002) p38 MAPK mediates the regulation of alpha1(I) procollagen mRNA levels by TNF-alpha and TGF-beta in a cell line of rat hepatic stellate cells(1). FEBS Lett. 528(1–3):133–8.

doi: 10.1016/S0014-5793(02)03276-3

[23] F. Xu, C. Liu, D. Zhou, L. Zhang (2016) TGF-β/SMAD Pathway and its regulation in hepatic fibrosis," J. Histochem. Cytochem. 64(3):157–167.

doi: 10.1369/0022155415627681

[24] A. M. Gressner, R. Weiskirchen, K. Breitkopf, and S. Dooley (2002) Roles of TGF-beta in hepatic fibrosis. Front. Biosci. 7:d793-807.

[25] M.R. de Galarreta , A. Navarro, E. Ansorena, A.G. Garzón, T. Mòdol, M.J. López-Zabalza, J.J. Martínez-Irujo, M.J. Iraburu (2016) Unfolded protein response induced by Brefeldin A increases collagen type I levels in hepatic stellate cells through an IRE1α, p38 MAPK and Smad-dependent pathway. BBA. Mol. Cell. Res. 1863:2115–2123.

doi:10.1016/j.bbamcr.2016.05.002

[26] M.F. Walsh, D.R. Ampasala, J. Hatfield, R. Vander Heide, S. Suer, A.K. Rishi AK,M.D. Basson (2008) Transforming Growth Factor-beta Stimulates Intestinal Epithelial Focal Adhesion Kinase Synthesis via Smad-and p38-Dependent Mechanisms. Am. J. Pathol. 173(2):385–399.

doi:10.2353/ajpath.2008.070729

[27] J. An, L. Zheng, S. Xie, Z. Dun, L. Hao, D. Yao, D.Q. Shih, X. Zhang (2011) Down-regulation of focal adhesion kinase by short hairpin RNA increased apoptosis of

rat hepatic stellate cells. APMIS. 119(6):319–329.

doi:10.1111/j.1600-0463.2011.02720.x

[28] G. Son, I. N. Hines, J. Lindquist, L. W. Schrum, and R. A. Rippe (2009) Inhibition of phosphatidylinositol 3-kinase signaling in hepatic stellate cells blocks the progression of hepatic fibrosis. Hepatology. 50(5):1512–1523.

doi: 10.1002/hep.23186.

[29] A. M. Bujor, J. Pannu, S. Bu, E. A. Smith, R. C. Muise-Helmericks, and M. Trojanowska (2008) Akt Blockade Downregulates Collagen and Upregulates MMP1 in Human Dermal Fibroblasts. J. Invest. Dermatol. 128(8):1906–1914.

doi: 10.1038/jid.2008.39

[30] T. G. Voloshenyuk, E. S. Landesman, E. Khoutorova, A. D. Hart, and J. D. Gardner (2011) Induction of cardiac fibroblast lysyl oxidase by TGF-beta1 requires PI3K/Akt, Smad3, and MAPK signaling. Cytokine. 55(1):90-7.

doi: 10.1016/j.cyto.2011.03.024

[31] T. Watanabe, H. Tajima, H. Hironori, H. Nakagawara, I. Ohnishi, H. Takamura, I. Ninomiya, H. Kitagawa, S. Fushida, T. Tani, T. Fujimura,T. Ota, T. Wakayama, S. Isek, and S. Harada (2011) Sodium valproate blocks the transforming growth factor TGF-β1 autocrine loop and attenuates the TGF-β1-induced collagen synthesis in a human hepatic stellate cell line. Int. J. Mol. Med. 28(6):919–925.

doi:10.3892/ijmm.2011.768

[32] R. Shah, K. Reyes-Gordillo, J. Arellanes-Robledo, C.G. Lechuga, Z. Hernández-Nazara, A. Cotty, M. Rojkind, M.R. Lakshman (2013) TGF-β1 up-regulates the expression of PDGF-β receptor mRNA and induces a delayed PI3K-, AKT-, and p70(S6K) -dependent proliferative response in activated hepatic stellate cells. Alcohol. Clin. Exp. Res. 37(11):1838–1848.

doi: 10.1111/acer.12167

[33] S. K. Mitra and D. D. Schlaepfer (2006) Integrin-regulated FAK–Src signaling in normal and cancer cells. Curr. Opin. Cell Biol. 18(5):516–523.

doi: 10.1016/j.ceb.2006.08.011

[34] P. Kumar,T. Smith, K. Rahman, J.E. Mells, N.E. Thorn, N.K. Saxena, F.A. Anania (2014) Adiponectin modulates focal adhesion disassembly in activated hepatic stellate cells: implication for reversing hepatic fibrosis FASEB J. 28(12):5172-83.

doi: 10.1096/fj.14-253229.

[35] X.K. Zhao, L. Yu, M.L. Cheng, P. Che, Y.Y. Lu, Q. Zhang, M. Mu, H. Li, L.L. Zhu, J.J. Zhu, M. Hu, P. Li, Y.D. Liang, X.H. Luo,Y.J. Cheng, Z.X Xu and Q. Ding (2017) Focal Adhesion Kinase Regulates Hepatic Stellate Cell Activation and Liver Fibrosis. Sci. Rep. 7(1):4032

doi: 10.1038/s41598-017-04317-0.

6. Acknowledgements

This work was supported by grants from *Plan de Investigación de la Universidad de Navarra* (PIUNA), Nottingham Trent University and FIS 16/01126 funding. Amaia

Navarro-Corcuera was supported by a predoctoral contract from “La Caixa Banking Foundation” and “*Asociación de Amigos de la Universidad de Navarra*”, and by mobility grants from *Gobierno de Navarra* and “Santander Banking Foundation”.

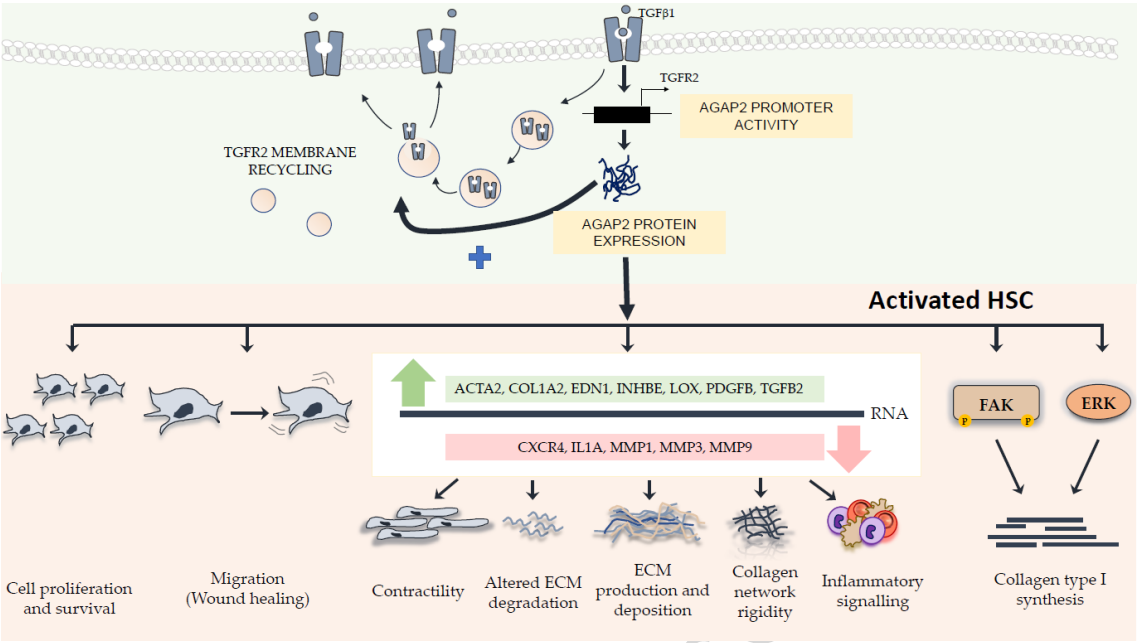

Graphical abstract

Highlights

1. AGAP2 mediates TGFβ1-induced viability, proliferative and migratory effects in HSC
2. AGAP2 is involved in the fibrogenic gene expression profile induced by TGFβ1 in HSC
3. TGFβ1 up-regulates AGAP2 promoter activity and protein expression in HSC
4. AGAP2 participates in the trafficking of the TGFR2 after TGFβ1 stimulation
5. AGAP2-mediated effect of TFGβ on collagen I expression requires FAK and ERK activity